PHYSICAL REVIEW B **81**, 241413(R) (2010)

Vector lensing with a single chain of metal nanoparticles

D. S. Citrin*

School of Electrical and Computer Engineering, Georgia Institute of Technology, Atlanta, Georgia 30332-0250, USA and Unité Mixte Internationale 2958 Georgia Tech-CNRS, Georgia Tech Lorraine, Metz Technopôle, 2 rue Marconi, 57070 Metz, France

(Received 12 March 2010; published 22 June 2010)

A *single* periodic chain of noncontacting noble-metal nanoparticles is predicted to provide focusing in a cylindrical geometry of optical fields whose frequency lies within the surface-plasmon-polariton band polarized perpendicular to the chain axis for fields dominated by that component based on an analytic nonlocal vector electrodynamic theory in the Fresnel limit. Exact closed-form expressions within the model for the coherently scattered field and the quadratic phase are obtained.

DOI: 10.1103/PhysRevB.81.241413 PACS number(s): 42.30.−d, 42.25.Gy, 78.67.Bf, 78.67.Pt

Since Pendry[1] predicted perfect lensing by a thin slab of negative-refractive-index (NRI) material, there has been a flurry of activity both in using metal films and slabs for perfect lensing as well as in the design and fabrication of appropriate metamaterials to achieve NRI.[2] Later several groups pointed out that periodic arrangements of noncontacting noble-metal nanoparticles (NPs) (Refs. 3 and 4) could give rise to NRI.[5–7] Kempa *et al.*[8] have shown that the intrinsic couplings within a simple periodic metal-nanoparticle lattice would lead to NRI effects.

The paradigm for understanding NRI effects is, namely, that: a refractive index with a negative value. As such, focusing by metal films or metamaterials is understood on the basis of the Fresnel equations, an intrinsically local electrodynamic theory (even if nonlocality has been taken into account in deriving a refractive index[9]). Indeed, for layers of thickness $\lesssim\lambda$, one expects nonlocality to enter from the start, and the very idea of a refractive index to be of limited validity. A more appropriate viewpoint is that an incident electromagnetic wave couples to material modes of the system whose group and phase velocities projected onto the material interface are in opposite directions.[1,8] The material modes then re-emit in a direction that appears as if the material possesses a NRI.

In the following, we show that indeed nonlocality is essential in nanoscale structures, choosing a chain of noncontacting noble-metal NPs that supports surface plasmon (SP) polaritons (SPP) as our test case. We predict that those spatial Fourier components of the electromagnetic field polarized transversely *T* with respect to the NP chain (NPC) axis can undergo focusing while longitudinal *L* components always suffer defocusing. These effects cannot be understood on the basis of a local electrodynamic theory phrased in terms of a refractive index.

The situation envisaged is shown in Fig. 1. A light source along a small length of arc of radius ρ (*object*) is to be imaged on a cylinder of radius ρ'. Thus, the problem breaks down into three parts: propagation from the object to the NPC, excitation of SPPs that radiate, and propagation from the NPC to the image. The free-space propagation will be treated in the Fresnel limit. The excitation of SPPs and their subsequent electromagnetic radiation will be treated within nonlocal vector electrodynamics.

We begin with the second task inasmuch as the first and third are well known and rather mechanically implemented. There are typically three types of SPPs in a NP array associated with the direction of the SP dipole moment. Depending on the lattice symmetry and the excitation wave vector $\mathbf{k}$, there are two transverse or *T* modes where the dipole moments are perpendicular to $\mathbf{k}$ and one longitudinal or *L* mode where the dipole moments are parallel to $\mathbf{k}$; only the *T* modes exhibit the requisite downward trend with increasing k in their dispersion curves. In practice, these modes may exhibit $\mathbf{k}$-dependent *LT* mixing, particularly in low-symmetry directions within the Brillouin zone.[10] The situation, however, simplifies for a one-dimensional system. Consider a NPC along the z axis embedded within a uniform dielectric. There are two *T*-modes and one *L*-mode.

SPPs in NPCs can be described[11] exactly, in the sense of accounting for the retarded vector electromagnetic field, treating the NPs as point dipoles within the coupled-dipole model.[12] Specifically, we consider a linear array of equispaced NPs (isotropic point dipoles) that interact with the retarded electromagnetic fields emitted by the other NPs and with an incident electromagnetic field $\mathbf{U}_1(nd)$ at the location $nd\hat{\mathbf{z}}$ of NP n, oscillating at frequency $\varepsilon/\hbar$ with ε the photon energy, $\hat{\mathbf{z}}$ a unit vector pointing along the NPC axis in the z direction, and $n \in \mathbb{Z}$; d is the center-to-center spacing between NPs. The NPC is assumed to be embedded in a uniform dielectric with refractive index n_{emb}. In a NPC of isotropic dipoles, because the *L* and the two *T* modes are decoupled, we can decompose $\mathbf{U}_1(nd)$ into components along these three directions and compute the NPC's response to each component separately. We shall assume this decom-

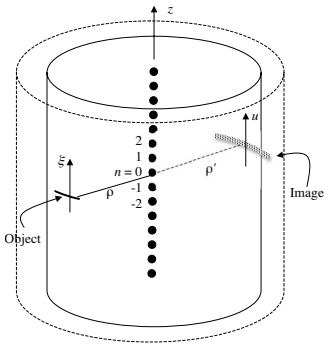

FIG. 1. Schematic of imaging geometry. Object lies on a cylinder of radius ρ and is imaged on a cylinder of radius ρ'. The nanoparticle chain lies on the concentric z axis of the cylinders; ξ and u measure the vertical coordinate on object and image cylinders, respectively.

 ©2010 The American Physical Society

position has been accomplished, thus producing a net response that may be simply obtained via superposition; the polarization index and the vector notation will henceforth be dropped. The dipole moment d_n on NP n is determined by $d_n=\alpha U_1(nd)+\chi\Sigma_{j=-\infty}^{\infty}\Sigma_{nj}d_j$, where the polarizability is $\alpha=p\chi$ with $\chi=2\varepsilon_0/(\varepsilon^2-\varepsilon_0^2+2i\varepsilon_0\gamma_{\rm nr})$ the susceptibility and $p=6\pi\epsilon_0(\hbar c)^3(2\gamma_{\rm r})/(n_{\rm emb}\varepsilon_0^3)$.[13] Here, ε_0 is the single-NP SP energy, $\gamma_{\rm nr}/\hbar$ is the single NP SP amplitude nonradiative decay rate, and ε_0 is the permittivity of free space. The radiative decay rate in the embedding dielectric is $\gamma_{\rm r}/\hbar=n_{\rm emb}\gamma_0/\hbar$ with $\gamma_0/\hbar$ the free-space value. These parameters were calculated in an electron-oscillator model[13] but p and $\gamma_{\rm r}$ may be regarded as adjustable parameters depending on the specific model employed. The radiative self-energy (SE) Σ_{nj} is the retarded dipole-dipole energy of dipoles n and j; detailed expressions are given in Ref. 11.

Due to the translational invariance of the problem, we can characterize the SPPs by the excitation wave vector k_z along the NPC axis. We take an incident field $U_1(nd)=u_0\exp(ink_zd)$ with u_0 a constant field amplitude. Such a field induces excitation[13]

$$d_n=d_0e^{ink_zd},\quad d_0=pu_0/(\chi^{-1}-\Sigma_{k_z}) \tag{1}$$

with exact closed-form expressions for the SE given in Ref. 11. The freely oscillating SPPs are found by setting $U_1(nd)=0$, which gives the PP dispersion relation $\chi^{-1}-\Sigma_{k_z}=0$.[11]

Our aim is to discuss the imaging properties of the NPC. To this end, we consider the electric field $\mathbf{U}_i(\mathbf{r}')$ at $\mathbf{r}'$ scattered by the NPC SPPs. We assume the cylindrical geometry as shown in Fig. 1. Write $\mathbf{U}_i(\mathbf{r}')=-\frac{\kappa^2}{4\pi\epsilon_0}\mathbf{u}_i(\mathbf{r}')$. Near the optical axis, we shall employ the Fresnel approximation, whereby we replace $\exp(i\kappa|\mathbf{r}'-\mathbf{r}_n|)/|\mathbf{r}'-\mathbf{r}_n|$ by $\frac{e^{i\kappa\rho'}}{\rho'}\exp[i\kappa(z'-nd)^2/(2\rho')]$ with ρ' the distance from the z axis in cylindrical coordinates. A detailed discussion of the validity of the Fresnel approximation is given in Ref. 14. Suffice it to say here that the Fresnel approximation is valid provided the object and image are sufficiently close to the optical axis when compared with ρ and ρ'. The Fresnel approximation is only used to propagate the field $U_O(\xi)$ from the object to the NPC and from the NPC to the image $U_I(u)$ as in Fig. 1; the SPPs within the NPC, however, are not computed within the Fresnel approximation and assume an infinitely long NPC. In the Fresnel limit $\mathbf{u}_i(n'd)=\mathbf{B}_i\frac{e^{i\kappa\rho'}}{\rho'}\Sigma_{n=-\infty}^{\infty}d_ne^{i\kappa d^2(n'-n)^2/(2\rho')}$, where $\mathbf{B}_L=\hat{\mathbf{z}}$ and $\mathbf{B}_T=\hat{\phi}$, $\mathbf{r}_n=nd\hat{\mathbf{z}}$ and $\kappa=\varepsilon n_{\rm emb}/(\hbar c)$ with c the *in vacuo* speed of light, and we restrict our attention to discrete locations with $z'=n'd$.

From our expression for d_n, we have for local excitation with field $U_1(nd)=u_0\delta_{0n}$ at (without loss of generality) $n=0$,

$$d_n=pu_0\frac{d}{\pi}\int_{-\pi/d}^{\pi/d}\frac{dk_z}{\chi^{-1}-\Sigma_{k_z}}e^{ink_zd}. \tag{2}$$

While exact expressions are available for Σ_{k_z},[11] their employment would render the integral above intractible.

We assume in effect a *static* nearest-neighbor dipole-dipole coupling, and neglect all other couplings.[4] In this case, $\Sigma_{k_z}=\frac{\Delta_j}{2}\cos k_zd$, where $j=L,T$ and $\frac{\Delta_j}{2}$ the SPP bandwidth for polarization j with $\Delta_L=-2\Delta_0$, $\Delta_T=\Delta_0$, and $\Delta_0/2=\gamma_{\rm r}/(\kappa d)^3$. For $n\geq 0$, Eq. (2) gives[15]

$$d_n=\frac{2\chi pu_0}{\pi}\int_0^{\pi}\frac{d\xi}{1+g\cos\xi}\cos n\xi=\frac{2\chi pu_0}{\sqrt{1-g^2}}\left(\frac{\sqrt{1-g^2}-1}{g}\right)^n \tag{3}$$

with $g=-\chi\Delta_j/2$. The main effect of this approximation is likely to be the neglect of the radiative losses (imaginary part of Σ_k whose scale is set by $\gamma_{\rm r}$) for $|k|<\kappa$. Inasmuch as $\gamma_{\rm r}$ is typically considerably less than $\gamma_{\rm nr}$, from the viewpoint of the imaging properties of NPCs, it is the nonradiative losses that are likely to play the leading role. To the extent $\gamma_{\rm nr}$ can be taken to be k independent, the inclusion of these losses is straightforward in the treatment below. Its two main effects are giving in effect a range of k values of SPPs excited by a monochromatic source (blurring the image) and also rendering invalid the final closed-form result for the quadratic phase we find below that provides the condition for an imaging geometry.

To proceed, put $e^{i\zeta}=(\sqrt{1-g^2}-1)/g$ $(n\geq 0)$. Within the SPP band, $|g|>1$. Note that $g=-\frac{\Delta_j}{2}(\varepsilon-\varepsilon_0+i\gamma_{\rm nr})^{-1}$, whence $\mathrm{sgn\,Im}\sqrt{1-g^2}=-\mathrm{sgn}\,\Delta_j$. Thus, $\sqrt{1-g^2}=\pm i\sqrt{g^2-1}$ for the L and T modes, respectively. We therefore have $e^{i\zeta}=\cos\zeta+i\sin\zeta=(\sqrt{1-g^2}-1)/g=\pm i\sqrt{1-g^{-2}}-g^{-1}$. For negligible $\gamma_{\rm nr}$, we can easily equate the real and imaginary parts of this expression. The real part gives $\zeta=\arccos(-g^{-1})$ while the imaginary part restricts ζ to $0\leq\pm\zeta\leq\pi$, again where the upper (lower) sign is for the L (T) mode. Rearranging $\zeta=\arccos(-g^{-1})$, we see that this is just the dispersion relation $\varepsilon-\varepsilon_0+i\gamma-\frac{\Delta_j}{2}\cos\zeta=0$. In other words, $\frac{\zeta}{d}$ is the wave vector satisfying the dispersion relation for excitation energy ε and further obeys $\zeta>0$ (<0) for L (T) modes, viz., SPPs whose phase velocity is traveling away from (toward) NP 0 are excited for L (T) polarized light.

For excitation outside the SPP band, $|g|<1$. Then $e^{i\zeta}=(\sqrt{g^{-2}-1}-g^{-1})$ and its reciprocal $e^{-i\zeta}=(-\sqrt{g^{-2}-1}-g^{-1})$. Forming $\cosh i\zeta$, we obtain either $i\zeta=\mathrm{arccosh}(-g^{-1})$ or $i\zeta=-\mathrm{arccosh}(-g^{-1})$. Only the second is consistent with $\zeta=-\arccos(-g^{-1})$ and $0\leq\pm\zeta\leq\pi$ for $|g|<1$.

Finally, consider the case when $n<0$. Then,

$$\begin{aligned}d_n&=\frac{2\chi pu_0}{\sqrt{1-g^2}}\left(\frac{\sqrt{1-g^2}-1}{g}\right)^{-|n|}\\&=\frac{2\chi pu_0}{\sqrt{1-g^2}}\left(\frac{-\sqrt{1-g^2}-1}{g}\right)^{|n|}.\end{aligned} \tag{4}$$

Consequently, $e^{i\zeta}=\cos\zeta+i\sin\zeta=(-\sqrt{1-g^2}-1)/g=\mp i\sqrt{1-g^{-2}}-g^{-1}$, whence for $n<0$, $\zeta=\arccos(-g^{-1})$ with $0\leq\mp\zeta\leq\pi$ for $|g|>1$ and $i\zeta=\mathrm{arccosh}(-g^{-1})$ for $|g|<1$.

This lengthy analytical discussion of the Eqs. (3) and (4) is of key importance; we see that for excitation frequencies within the SPP band, if the polarization is L (T), then resonant SPPs are excited with phase velocity away from (toward) the point of excitation, while for excitation outside the SPP band, the SPPs excited decay exponentially away from

the point of excitation. While in the foregoing discussion, we took $\gamma_{\rm nr}$ to be negligibly small, the beauty of the analysis is that it applies for non-negligible $\gamma_{\rm nr}$ as well.

With reference to Fig. 1, assume, as stated above, the object field $U_O(\xi)$ is a short arc source on the circumference of the cylinder of radius ρ at $\xi=0$. We will use the Fresnel approximation to propagate the object field $U_O(\xi)$ to the NPC and from the NPC to the image field $U_I(u)$, where ξ and u are the vertical coordinates on the object and image cylinders. We shall not be concerned about the ϕ dependence. Since fields near the optical axis are of main import, we can assume that fields coupled to the L (T) modes only produce fields on the image cylinder polarized in the u (ϕ) direction.

In view of the above, we have $U_1(z)=u_0 1/i\lambda\rho e^{i\kappa\rho}\exp[i\kappa/2\rho(z-\xi)^2]$. Then, $U_2(n'd)=\Sigma_{n=-\infty}^{\infty}U_1(nd)d_n$, giving

$$U_2(n'd) = -\frac{\kappa^2}{4\pi\epsilon_0}u_0 e^{i\kappa\rho}\frac{2p\chi}{i\lambda\rho\sqrt{1-g^2}} \times \sum_{n=-\infty}^{\infty} e^{i(\kappa/2\rho)(nd-\xi)^2}e^{i|n'-n|\zeta} \tag{5}$$

with ζ for $n>0$. Further propagating the field to the image cylinder gives the point spread function $h(u,\xi)$ for the imaging system given an arbitrary object field $U_O(\xi)$ as $U_I(u)=\int d\xi h(u,\xi)U_O(\xi)$ with[14]

$$\begin{aligned} h(u,\xi) &= \frac{\kappa^2}{4\pi\epsilon_0}\frac{2p\xi}{\lambda^2\rho\rho'\sqrt{1-g^2}}e^{i\kappa(\rho+\rho')} \\ &\times \sum_{n,n'=-\infty}^{\infty} e^{i(\kappa/2\rho')(n'd-u)^2}e^{i|n'-n|\zeta}e^{i(\kappa/2\rho)(nd-\xi)^2} \\ &= \frac{\kappa^2}{4\pi\epsilon_0}\frac{2p\xi}{\lambda^2\rho\rho'\sqrt{1-g^2}}e^{i\kappa(\rho+\rho')}e^{i(\kappa/2)(u^2/\rho'+\xi^2/\rho)}\sum_{n,n'=-\infty}^{\infty} \\ &\times e^{-i(\kappa d/\rho')n'u}e^{i(\kappa d^2/2\rho')n'^2}e^{i|n'-n|\zeta}e^{-i(\kappa d/\rho)n'\xi}e^{i(\kappa d^2/2\rho)n^2}. \end{aligned} \tag{6}$$

Equation (6) is key to our study. Let us consider it factor by factor. The prefactor $\frac{\kappa^2}{4\pi\epsilon_0}\frac{2b\xi}{\lambda^2\rho\rho'}(1-g^2)^{-1/2}e^{i\kappa(\rho+\rho')}$ does not contain any variation in the vertical direction and thus we consider it no further. The quadratic phase factors $e^{i(\kappa/2)(u^2/\rho')}$ and $e^{i(\kappa/2)(\xi^2/\rho)}$ will be neglected as these phases can be corrected for by suitable curvature of the object and image surfaces in the vertical direction.[14] Finally, we are left with the factor of interest, viz., the double summation. Put $\nu=n'-n$ and $N=\frac{n'+n}{2}$; we can rewrite the summation in Eq. (6) as

$$\begin{aligned} &\sum_{\nu,N=-\infty}^{\infty} e^{-i(\kappa d/\rho')(N+\nu/2)u}e^{i(\kappa d^2/2\rho')(N+\nu/2)'^2} \\ &\times e^{i|n'-n|\zeta}e^{-i(\kappa d/\rho)(N-\nu/2)\xi}e^{i(\kappa d^2/2\rho)(N-\nu/2)^2} \\ &= \sum_{N=-\infty}^{\infty} e^{-i\kappa dN(u/\rho'+\xi/\rho)}J_N, \end{aligned} \tag{7}$$

$$\begin{aligned} J_N &= e^{i(\kappa d^2/2)(1/\rho'+1/\rho)N^2}\sum_{\nu=-\infty}^{\infty} e^{-i(\kappa d/2)(u/\rho'-\xi/\rho)\nu} \\ &\times e^{i|\nu|\zeta}e^{i(\kappa d^2/2)(1/\rho'-1/\rho)N\nu}e^{i(\kappa d^2/8)(1/\rho'+1/\rho)\nu^2}. \end{aligned} \tag{8}$$

To characterize the imaging properties of the NPC, we need to extract the quadratic phase q (proportional to N^2) in J_N, i.e., obtained from the phase factor e^{iqN^2}. One such phase factor appears explicitly, viz., $e^{i(\kappa d^2/2)(1/\rho'+1/\rho)N^2}$. Other contributions are contained within the summation in J_N. Thus, we seek to isolate the quadratic phase factor in J_N of the form $e^{-i(\kappa d^2/2)(1/f)N^2}$, where f is the focal length, should it exist, for which the lens equation $\frac{1}{\rho}+\frac{1}{\rho'}=\frac{1}{f}$ holds.

In evaluating J_N, we shall neglect the u- and ξ-dependent factors (assuming the object and image are close to the optical axis) and further we shall make a long-wavelength approximation, whereby the summation over ν is replaced by an integration. This should be valid so long as the nanoparticle center-to-center spacing $d\ll\frac{2\pi}{\kappa}$ and we are not interested in values of ζ too close to $\pm\pi$. The main effect of d in the long-wavelength approximation is simply to determine the SPP bandwidths $\frac{\Delta_j}{2}$ as given above in the expression for Δ_0. Thus, the smaller d, the larger the SPP bandwidths, and thus the easier it is to select the resonant SPP wave vector in the presence of the inevitable $\gamma_{\rm nr}>0$ by a monochromatic source. Small d is thus desirable. (Moreover, small d implies a large oscillator strength associated with the SPPs, and thus the scattered field of interest will be enhanced.) If the long-wavelength approximation is not satisfied, the discreteness of the NPC becomes important and the summations can no longer be approximated as integrals. The NPC then acts as a grating rather than a metamaterial, and will produce pronounced diffraction orders in $U_I(u)$, which in an imaging context will be undesirable artifacts. Putting $\beta=\frac{\kappa d}{8}(\frac{d}{\rho'}+\frac{d}{\rho})$ and $b=\frac{\kappa d}{2}(\frac{d}{\rho'}-\frac{d}{\rho})$ (N.B., $|b|\le 4\beta$), we have

$$\begin{aligned} J_N &\approx \frac{2}{d}e^{4i\beta N^2}\int_0^{\infty} dy e^{i\zeta y/d}e^{i\beta y^2/d^2}\cos\frac{bNy}{d} \\ &= \frac{1}{2}\sqrt{\frac{\pi}{i\beta}}e^{4i\beta N^2}\left[e^{(i\zeta-ibN)^2/4i\beta}\,\mathrm{erfc}\left(\frac{i\zeta-ibN}{2\sqrt{i\beta}}\right)\right. \\ &\left. + e^{(i\zeta+ibN)^2/4i\beta}\,\mathrm{erfc}\left(\frac{i\zeta+ibN}{2\sqrt{i\beta}}\right)\right] \end{aligned} \tag{9}$$

with erfc the complementary error function.

Setting the quadratic phase $q(\zeta)=4\beta+\lim_{N\to 0}[\arg(J_N)-\arg(J_0)]/N^2$ to zero determines those excitation wave vectors ζ (surrogate for frequencies) for which the image is in focus for a given geometry characterized by β and b. The limit can be carried out as follows. First, expand Eq. (9) in powers of N, viz., $J_N\approx J_0(1-\frac{b^2N^2}{2}j_2/J_0)$ with $j_2=2\int_0^{\infty}dx x^2e^{i\zeta x}e^{i\beta x^2}=-i\frac{\partial}{\partial\beta}J_0$. Both J_0 and j_2 can be expressed in closed form by lengthy expressions (not given here) involving error functions. From the above, one then has $q(\zeta)=4\beta+\lim_{N\to 0}[\arg(J_0)+\arg(1-\frac{b^2N^2}{2}\frac{j_2}{J_0})-\arg(J_0)]/N^2=4\beta+\lim_{N\to 0}\arg(1-\frac{b^2N^2}{2}\frac{j_2}{J_0})/N^2$. We have $\lim_{N\to 0}\arg(1$

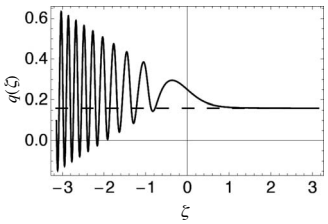

FIG. 2. Quadratic phase $q(\zeta)$ in z direction as a function of the excitation wave vector ζ resonant with the object ε. Horizontal dashed line shows quadratic phase associated with propagation from object to nanoparticle chain on the z axis, and from nanoparticle chain to image; thus, it does not account for the effect of the nanoparticle chain. Values of $\zeta>0$ correspond to L-polarized component of object while $\zeta<0$ corresponds to T-polarized component. When $q(\zeta)=0$, focusing of T-polarized component occurs.

$-\frac{b^2N^2}{2}\frac{j_2}{J_0})/N^2 = \mathrm{Im}\ \ln(1-\frac{b^2N^2}{2}\frac{j_2}{J_0})/N^2 = -\frac{b^2N^2}{2}\mathrm{Im}(\frac{j_2}{J_0})/N^2 = -\frac{b^2}{2}\mathrm{Im}\times(\frac{j_2}{J_0})$. This can be simplified as $q(\zeta)=4\beta+b^2/4\beta+b^2\zeta/4\beta\sqrt{\pi}\mathrm{Im}[\exp(-i\zeta^2/4\beta)/\sqrt{i\beta}\mathrm{erfc}(i\zeta/2\sqrt{i\beta})]$.

In Fig. 2 is plotted $q(\zeta)$ for $\beta=0.04$ and $|b|=3\beta$. What we are looking for are values of ζ (excitation wave vectors, in turn energies) such that $q(\zeta)=0$ for which the lens equation is satisfied and an image is formed. Note that for $\zeta>0$ (i.e., the L modes), $q(\zeta)>0$, from which we conclude that a L-polarized object does not form an image; the defocusing effect of L modes is rather weak compared with the free-space quadratic phase 4β. Nonetheless, whether $q(\zeta)<4\beta$ or $q(\zeta)>4\beta$ predicts whether the NPC acts in effect as a converging or diverging lens. Recall, $|b|\leq 4\beta$, and based on Eq. (9), J_N and thus $q(\zeta)$ are independent of the sign of b, and consequently the focusing is symmetric (which is not surprising), viz., if (ρ,ρ') is a focusing geometry, so is (ρ',ρ). When $|b|$ is at its maximum value, the amplitude of the oscillations in $q(\zeta)$ that increase with decreasing ζ reaches its maximum. Since β sets the value these oscillations must overcome to give $q(\zeta)=0$, focusing geometries favor small β and large $|b|$; we find $\beta\lesssim 0.154$ with $|b|=4\beta$ is the maximum value of β to result in focusing, for which $\zeta=-\pi$. When focusing occurs, the total quadratic phase vanishes, and thus from the lens equation we can write down a focal length; however, this cannot be interpreted as *the* focal length in the usual sense of the NPC since when this occurs itself depends on ρ. Our discussion of the limited cases here is only approximate; since we have made the long-wavelength approximation, our results can only serve as a rough guide for $|\zeta|\sim\pi$. Also note that $\beta\propto\frac{1}{\rho}+\frac{1}{\rho'}$ while $b\propto\frac{1}{\rho}-\frac{1}{\rho'}$; $|b|=4\beta$ means either ρ or $\rho'=0$ or ∞. Finally, once the desired value of ζ is found for T-polarized focusing to occur, the corresponding value of the excitation energy ε can be obtained.

To conclude, we have presented a treatment of the imaging properties of a NPC in a cylindrical geometry chosen to provide an analytically tractable model for vector lensing effects in NP structures. A focusing effect is predicted for monochromatic fields within the T SPP band. Limitations to the resolution are expected due to γ_{nr} and its role in spreading out in k space the range of resonant SPPs excited by a monochromatic source. In the foregoing numerical examples, we did not include γ_{nr}, though all the expressions except the final one for $q(\zeta)$ remain valid; then $\zeta\in\mathbb{C}$. As the value of β is decreased, there are an increasing number of values of ζ for which $q(\zeta)<0$; thus the ability to choose a narrow range of excitation wave vectors ζ by varying energy ε will be reduced by the inclusion of γ_{nr} (though this effect can be taken into account using the above expressions). Consequently, chromatic aberration will be severe and fairly monochromatic objects will be required. Other questions left unexplored are going beyond the long-wavelength and Fresnel approximations, higher-order phases (that may limit the image formation to unreasonably small objects), and the role of the neglected u- and ξ-dependent phases. Finally, we have not considered the artifact associated with the nonscattered portion of the incident object field.

*david.citrin@ece.gatech.edu

[1] J. B. Pendry, Phys. Rev. Lett. **85**, 3966 (2000); J. B. Pendry *et al.*, *ibid.* **76**, 4773 (1996).
[2] C. M. Soukoulis *et al.*, Science **315**, 47 (2007).
[3] M. Quinten *et al.*, Opt. Lett. **23**, 1331 (1998).
[4] S. A. Maier *et al.*, Appl. Phys. Lett. **81**, 1714 (2002).
[5] N. Engheta *et al.*, Phys. Rev. Lett. **95**, 095504 (2005); A. Alù *et al.*, Opt. Express **14**, 1557 (2006).
[6] L. Liu *et al.*, J. Appl. Phys. **92**, 5560 (2002).
[7] C. Mateo-Segura, C. R. Simovski, G. Goussetis, and S. Tretyakov, Opt. Lett. **34**, 2333 (2009); S. A. Tretyakov *et al.*, J. Opt. Soc. Am. A **17**, 1791 (2000); P. Alitalo *et al.*, Phys. Rev. B **74**, 235425 (2006).
[8] K. Kempa *et al.*, Phys. Rev. B **72**, 205103 (2005).
[9] R. Ruppin *et al.*, Phys. Rev. B **72**, 153105 (2005).
[10] T. D. Backes *et al.*, Phys. Rev. B **78**, 153407 (2008); IEEE J. Sel. Top. Quantum Electron. **14**, 1530 (2008).
[11] D. S. Citrin, Nano Lett. **4**, 1561 (2004); Opt. Lett. **31**, 98 (2006).
[12] E. M. Purcell *et al.*, Astrophys. J. **186**, 705 (1973); V. A. Markel, J. Mod. Opt. **40**, 2281 (1993).
[13] D. S. Citrin *et al.*, J. Opt. Soc. Am. B **25**, 937 (2008).
[14] J. W. Goodman, *Introduction to Fourier Optics* (Roberts, Englewood, Colorado, 2005).
[15] B. De Haan, *Nouvelles tables d'intégrales définies* (G. E. Stechert, New York, 1939).